Brackish springs in coastal aquifers and the role of calcite dissolution by mixing waters

Esteban Sanz Escudé

October 19, 2007

CHAPTER 2: MECHANISMS OF SALINIZATION OF COASTAL BRACKISH SPRINGS

PhD Thesis
Department of Geotechnical Engineering and Geo-Sciences (ETCG)
Technical University of Catalonia (UPC)

Supervisors:
Dr. Jesús Carrera Ramírez
Dr. Carlos Ayora Ibáñez

Institute of Earth Sciences 'Jaume Almera', CSIC

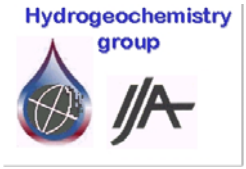

Chapter 2

Mechanisms of salinization of coastal brackish springs

Advances in science have overturned the belief of the ancient Greeks that seawater, consisting of water and earth (two of the five basic elements), flowed inland where its earthen component slowly returned to its natural state giving rise to fresh groundwater. It is believed that this concept originated in the Island of Cephallonia (Greece) as a result of the simultaneous observation of a continuous flow of seawater into carbonate rocks on the west side of the island, and the cloud frequency over the island's mountains (Stringfield and LeGrand, 1969). The particular phenomenon of Cephallonia triggered a scientific controversy that would last for centuries. A number of imaginative but often physically unacceptable hypotheses had been advanced to account for the phenomenon (Fouqué, 1867; Wiebel, 1874, in Breznick, 1973; Crosby and Crosby, 1896; and Fuller, 1907) until Maurin and Zoetl (1967) demonstrated with a colouring test that the inflowing seawater returned to the surface in brackish karst springs located at a distance of 15 km from the opposite side of the island.

Brackish springs are relatively frequent phenomena in coastal carbonate formations and their existence has been extensively reported, especially in the Mediterranean area (Payne et al., 1978, reviews of Breznik, 1973; Leontiadis et al., 1988; and Fleury et al., 2007a) In fact, more than 300 springs have been identified in the coast of former Yugoslavia (Bonacci and Roje-Bonacci, 1997). They essentially consist of inland or submarine karst outlets discharging waters with flow-dependent salinity. The phenomenon is particularly surprising in inland springs. They

may discharge high flow rates with significant salinities (presumably coming from the sea) at elevations of several meters above sea level, which reveals the especial complexity of their hydraulic and salinization mechanisms. Although these phenomena have been studied for many years, controversy persists.

The occurrence of a well-developed deep karst system in a seawater intrusion zone appears to be the key factor in the formation of brackish springs (Mandel, 1971). As a result of tectonic constraints and different variations in the sea level over a geological time scale, a series of stacked karstic drainage networks could be generated (Fleury et al., 2007a). Moreover, mixing of fresh and seawater may lead to carbonate dissolution (Rezaei et al., 2005) further enlarging the conduit section at depth and modifying the seawater intrusion pattern. Under these conditions, a plausible scenario consists of a karst conduit open directly to the sea, allowing mixing at a deep conduit branching. The concept of conduit branching (or branching point) as a structure controlling the functioning of salty springs was first introduced by Breznik (1973). The conduit branching is the junction of three conduits: one with freshwater, another one connected to the sea, and the third one with brackish water leading to the spring mouth (Figure 2.a). In fact, such conduit branching has never been directly observed, and the uncertainties associated with its potential geometry and dimensions have led authors to propose different physical mechanisms to explain the phenomenon. The proposed mechanisms of salinization can be divided into two groups (Stringfield and LeGrand, 1969): salinization due to hydrodynamic effects and salinization due to the greater density of seawater. The first group involves physical conditions of flow in tubular openings or other channels which serve as Venturi tubes. This requires a narrowing of the freshwater conduit at the intersection with the seawater one, allowing the freshwater flowing through to cause a depression that sucks in seawater. This mechanism has been proposed for springs showing a rising or steady salinity with increasing discharge flow, such as the Slanac spring (Croatia) (Breznik, 1973) and the Makaria spring (Greece) (Maramathas and Boudouvis, 2006). However, these situations would require very high groundwater velocities and particular conduit networking morphologies that would be difficult to find in nature or to maintain without erosion. The second group of proposed mechanisms assumes that water becomes brackish at the conduit branching when the pressure in the upwards brackish water conduit is less than the pressure in the seawater tube. This situation becomes possible if the depth of the branching point is large enough to balance the elevation of the spring mouth with the reduced density of brackish water as compared to seawater. The variation of freshwater pressure with changes in freshwater flow in the aquifer would explain the salinity variation of the spring discharge (Gjurasin, 1943, and Kuscer, 1950, in Breznik, 1973). This mechanism has been widely accepted for springs that display an inverse relation of flow discharge with respect to salinity, i.e., discharging freshwater during high flows and, below a certain flow-limiting value, gradually more saline waters with decreasing

discharge. Examples include Almyros of Heraklion spring (Crete, Greece) (Breznik, 1973) and Blaz spring (Croatia) (Bonacci and Roje-Bonacci, 1997).

In some cases, geological constraints indicate that seawater contamination of freshwater flowing through a karst conduit would not be necessarily related to a conduit network connected directly to the sea, but rather to a diffusive seawater intrusion from the porous matrix surrounding the conduit (Arfib and de Marsily, 2004). This situation may occur when a freshwater conduit crosses a saline-intruded fissured matrix zone. Arfib and Ganoulis (2004) performed laboratory experiments demonstrating that a considerable mass exchange may happen under these conditions. It is not easy to confirm the most dominant mechanism of seawater intrusion in a specific case. This is because the geology at depth in coastal carbonate aquifers that present brackish springs is poorly documented. Nevertheless, modeling could provide some insight into the mechanisms of seawater influence in brackish springs.

There have been attempts to apply numerical models to brackish springs. They have been prompted by the fact that the discharge of those springs represents a precious resource in areas with limited water resources. Modeling proves to be an important tool to test different options of spring development proposed in the last decades (Breznik, 1973, Breznik, 1988, Leontiadis et al. 1988, Bonacci and Roje-Bonacci, 1997, Cardoso, 1997, Sanz et al., 2003). Some authors have employed nonlinear analysis or inverse modeling to calculate unit hydrographs and impulse responses from rainfall data in the recharge area (Lambrakis et al., 2000, Pinault et al., 2004). This type of models, extensively used for freshwater karst springs, use box reservoirs to represent the relationship between an input and an output signal. However, these methods do not take into account the physical processes and mechanisms controlling the spring functioning and therefore are not considered relevant for our study. Maramathas et al. (2003) proposed a different approach based on the mass and mechanical energy balance on a hydrodynamic analog, which included three reservoirs flowing from tubes lying adjacent to the spring. Two reservoirs emulate the karstic system (two karst subsystems with different depletion period), and the third one emulates the sea. This model assumes the existence of a conduit branching with a conduit open directly to the sea (although this is not simulated), and computes discharge and chloride concentration of the spring using rainfall data as model input. Although the model was successfully applied to the Almyros spring of Heraklion, transport, mixing at the conduit branching and the variable-density turbulent flow in conduits were not considered. In fact, the equations governing variable-density turbulent flow have never been addressed before. These equations, we believe, are crucial for a full understanding of the physics of spring functioning. In contrast to this work, Arfib and de Marsily (2004) applied a different conceptual model to the same spring. They assume the existence of a single freshwater conduit surrounded by a saline porous matrix, where salinization of freshwater in the conduit is a consequence of saline flux from the matrix. This considers constant-density

turbulent flow in the conduits and mass exchange ratio driven by the head difference between the conduit and the matrix. Surprisingly, these two studies at Almyros provided similar results even though they are based on rather different conceptual models and approaches. Therefore, a detailed description of these conceptual models for brackish springs and a direct comparison among them should be addressed.

The objectives of this study are (1) to derive the equations governing turbulent flow for density-dependent fluids, (2) to describe the salinization mechanisms of inland brackish springs presenting a connection with the sea through an open karst conduit or a diffusive seawater intrusion, and (3) to compare the spring discharge and concentration response with these two salinization mechanisms.

2.1. Theory

2.1.1. Conceptual models of brackish springs

Any conceptual model proposed to explain the functioning of brackish springs must include the existence of a well developed deep karst system and identify the dominant mechanism of seawater contamination, i.e., the way in which seawater intrudes into the aquifer and mixes with freshwater. This work is focussed on two conceptual models that we consider are the most plausible ones to occur in nature (Figure 2.1 and Figure 2.2). Both conceptual models can explain inverse relations of concentration and discharge of inland springs, but applying different salinization mechanisms. The first conceptual model, Turbulent-Turbulent (T-T), assumes that the groundwater circulates only through a network of conduits and that the seawater contamination occurs at a deep conduit branching through a conduit open directly to the sea (Figure 2.1). Note that dashed conduit in Figure 2.1 and Figure 2.2 represents a conduit of undefined shape connecting with the sea. In these environments groundwater flow follows the hydraulic laws for pipes, and the flow can be laminar or turbulent depending on the velocity of the fluid, the properties of the fluid, and the shape and extend of the conduit section (Chadwick and Morfett, 1998). This problem can be simplified into a mass and energy balance at the conduit branching. When the interface between the freshwater and seawater is placed at the conduit branching, mixing of two waters of variable density takes place (Figure 2.1a). If the freshwater flow reaching the conduit branching is high enough, freshwater can intrude into the conduit connected to the sea, pushing the water contained in it seawards and creating a submarine spring on the sea floor (Figure 2.1b). By contrast, if the freshwater flow is very low (or eventually zero) the seawater will intrude into the conduit with freshwater thus increasing the seawater contamination in the aquifer.

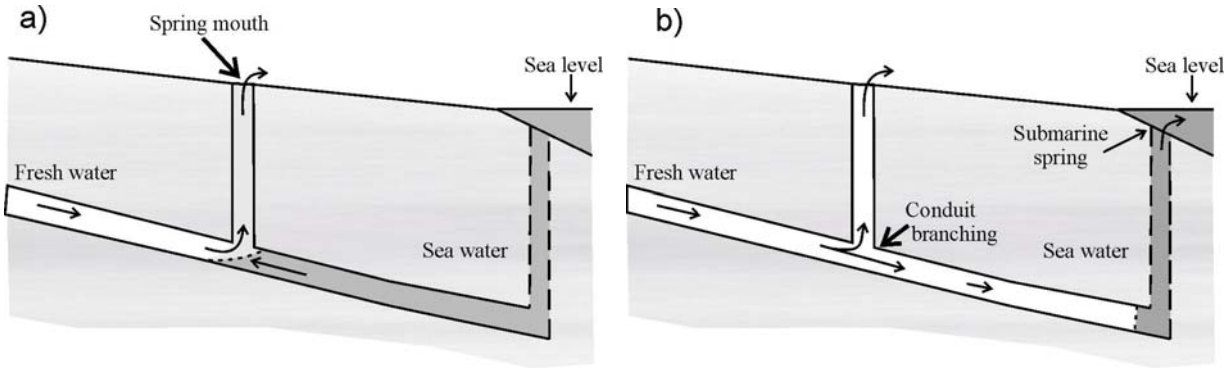

Figure 2.1: Scheme of the Turbulent-Turbulent conceptual model for brackish springs that considers salinization from seawater through a conduit open directly to the sea. Two situations are shown: a) mixing of waters is produced at the conduit branching and the spring discharges brackish water; and b) high freshwater flow intrudes into the conduit connected to the sea, thus creating a submarine spring on the sea floor. Textured grey areas represent the (low permeability) matrix. Water salinity in the conduits increases from white to dark grey.

The second conceptual model for spring salinization explored in this study, called Turbulent-Porous (T-P), combines the existence of a conduit network immersed in a fissured matrix. It considers that an open conduit crossing a fissured matrix intruded by seawater will become contaminated by diffusive mass transfer from the matrix (Figure 2.2) (Arfib and de Marsily, 2004).

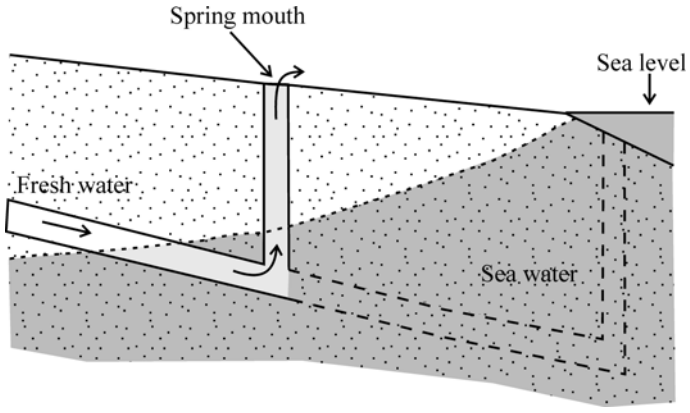

Figure 2.2: Scheme of the Turbulent-Porous conceptual model for brackish springs that considers salinization from seawater by diffuse exchange between the conduit and the surrounding porous matrix. Dotted areas represent the porous/fissured matrix. Water salinity in the conduit and the matrix increases from white to dark grey.

Given the complexity of karst systems, the schemes of Figure 2.1 and Figure 2.2 should be viewed as modeling simplifications. Combinations of multiple conduit branchings contaminated

at different points are likely to occur in natural systems. Nevertheless, these models further our understanding of the physics controlling the phenomenon, which is the aim of this study.

2.1.2. Governing equations

Both conceptual models considered in this study consist of a mixing place in which a conduit connected to the sea and another conduit from the aquifer inland, join a third vertical conduit with mixed water leading to the spring mouth. But, depending on the conceptual model, the seawater conduit is assumed to be an open conduit (T-T case) or a porous/fissured medium (T-P case) (Figure 2.1 and Figure 2.2, respectively). In both cases flow is governed by mass and either momentum or energy conservation. We found no equations for variable density pipe flow. Therefore, they are derived below.

To express these conservation principles let us consider a conduit with open area A_l ($A = A'\phi$, where A' is the total area and ϕ porosity, in the case of a porous medium), where l is the length along the conduit axis. Fluid mass conservation is expressed as:

$$\frac{\partial \rho A}{\partial t} = -\frac{\partial \rho A v}{\partial l} \tag{2.1}$$

where $\rho = \rho(l,t)$ is density and $v = v(l,t)$ is velocity.

Momentum conservation can be expressed in lagrangian coordinates, in which case it expresses Newton's second law, or in eulerian coordinates. We adopt the second option, which implies that the variation of momentum ($\frac{\partial \rho A v}{\partial t}$) is equal to the inflow minus outflow of momentum per unit length of conduit ($-\frac{\partial \rho A v^2}{\partial l}$) plus the forces acting in the fluid (expressed per unit length: $-\frac{\partial PA}{\partial l} - \rho A g \cos\theta - f_P$, where $\cos\theta = \partial z/\partial l$ and f_P represents the component of the forces exerted by the conduit walls over the fluid). That is,

$$\frac{\partial \rho A v}{\partial t} = -\frac{\partial \rho A v^2}{\partial l} - \frac{\partial PA}{\partial l} - \rho A g \cos\theta - f_P \tag{2.2}$$

This equation can be used, together with eq (2.1), for solving the problem. However, we prefer to write the equations in terms of energy, which is the traditional approach in hydraulics. To this end, we expand the time derivative, use eq (2.1) to eliminate the resulting $\partial \rho A/\partial t$ and perform some minor algebraic manipulations to obtain

$$\rho A \frac{\partial v}{\partial t} = -\left(\rho A \frac{\partial v^2/2}{\partial l} + \frac{\partial PA}{\partial l} + \rho A g \cos\theta + f_P \right) \tag{2.3}$$

Multiplying eq (2.3) by v and adding eq (2.1) multiplied by $v^2/2$, yields (after some algebraic operations):

$$\frac{\partial \rho A v^2/2}{\partial t} = -\left[\frac{\partial}{\partial l}\left(\rho A \frac{v^3}{2}\right) + v\frac{\partial PA}{\partial l} + \rho A v g\cos\theta + f_P v\right] \quad (2.4)$$

This equation is still not easy to apply because of the pressure forces exerted by the conduit walls. These can be ignored if A is assumed to be constant. Moreover, measurements are rarely more frequent than hourly so that pressure waves can be ignored and the fluid is assumed to be incompressible, so that Q (Av) is constant along the conduit. With these simplifications, eq (2.4) becomes

$$-\frac{1}{Q}\frac{\partial \rho A v^2/2}{\partial t} = \frac{\partial}{\partial l}\left(\rho\frac{v^2}{2} + P\right) + \rho g\cos\theta + \frac{f_P}{A} \quad (2.5)$$

Equation (2.5) resembles Bernouilli's equation except for the fact that ρ varies in space and time in response to variations in the proportion of seawater. Integrating eq (2.5) along the conduit, while ignoring kinetic energy variations, leads to:

$$(\rho_2 - \rho_1)\frac{v^2}{2} + P_2 - P_1 + \overline{\rho} g(z_2 - z_1) + \frac{\overline{f_P} L}{A} = 0 \quad (2.6)$$

Where the overbar stands for spatial average, z is the depth, and L is the conduit length between points 1 and 2. The only difference between the open and the porous conduits stems from the expression of $\overline{f_P}$. In the case of the open conduit, we have used Manning's equation:

$$\overline{f_P} = \frac{n^2 \overline{\rho} g Q^2}{A R_H^{4/3}} \quad (2.7)$$

where n is Manning's coefficient and R_H is the hydraulic radius of the conduit (ratio of A to wet perimeter). In the case of porous medium, $\overline{f_P} = A\mu v/k$, where μ is viscosity (assumed constant and equal to 1x10^{-3} m s/kg) and k intrinsic permeability. This, together with neglecting v^2, yields Darcy's law:

$$v = \frac{k}{\mu}\left(\frac{P_1 - P_2}{L} + \frac{\overline{\rho} g(z_1 - z_2)}{L}\right) \quad (2.8)$$

The fact that ρ varies in space and time forces us to solve the salt mass conservation equation, which we have written (neglecting dispersion) as:

$$\frac{\partial c}{\partial t} = -v\frac{\partial c}{\partial l} \quad (2.9)$$

where c is salt mass fraction (equal to 3.57x10^{-2} for seawater). Density depends on concentration as:

$$\rho = \rho_0 \exp(\alpha c) \quad (2.10)$$

where ρ_0 is the density of pure water (1000 kg/m^3) and α equals 0.69167 for mixtures of pure and seawater. It should be noted that having assumed the cross section to be constant and the

fluid to be incompressible, the fluid mass conservation is equivalent to solute mass conservation. This can be easily checked by plugging eq (2.10) into eq (2.1), which leads to eq (2.9).

Solution of these equations also requires specifying boundary conditions and continuity at the branching point. Pressure is specified as equal to atmospheric pressure (zero relative pressure) at the spring mouth. Energy (per unit volume) is specified at the seawater entry point

$$H_s = -\rho_s g z_s = P_s + \rho_s v_s^{\,2}/2 \tag{2.11}$$

where the subindex s stands for seawater entry point (or conduit). See Figure 2. for symbols. Continuity at the branching conduit is established in terms of fluid mass, solute mass and energy. That is

$$Q_m \rho_m = Q_f \rho_f + Q_s \rho_s \tag{2.12}$$

$$Q_m \rho_m c_m = Q_f \rho_f c_f + Q_s \rho_s c_s \tag{2.13}$$

and

$$H_{Bm} = H_{Bs} \tag{2.14}$$

where the subindex f stands for freshwater and m for mixed water. H_{Bm} and H_{Bs} result from eq (2.6) as:

$$H_{Bm} = P_{Bm} + \rho_{Bm}\frac{v_m^{\,2}}{2} = \overline{\rho}_m g L_m \left(1 + \frac{n_m^{\,2} Q_m^{\,2}}{A_m^{\,2} R_H^{\,4/3}}\right) + \rho_{m-spring} g \frac{v_m^{\,2}}{2} \tag{2.15}$$

and

$$H_{Bs} = P_{Bs} + \rho_{Bs}\frac{v_s^{\,2}}{2} = \rho_s g \left(-z_s - \frac{\overline{\rho}_s}{\rho_s}(z_B - z_s) - \frac{\overline{\rho}_s}{\rho_s}\frac{Q_s^{\,2} n_s^{\,2} L_s}{A_s^{\,2} R_H^{\,4/3}}\right) \tag{2.16}$$

for turbulent flow, or

$$H_{Bs} = \rho_s g \left(-z_s - \frac{\overline{\rho}_s}{\rho_s}(z_B - z_s) - \frac{Q_s \mu}{A_s k}\right) \tag{2.17}$$

for Darcy flow.

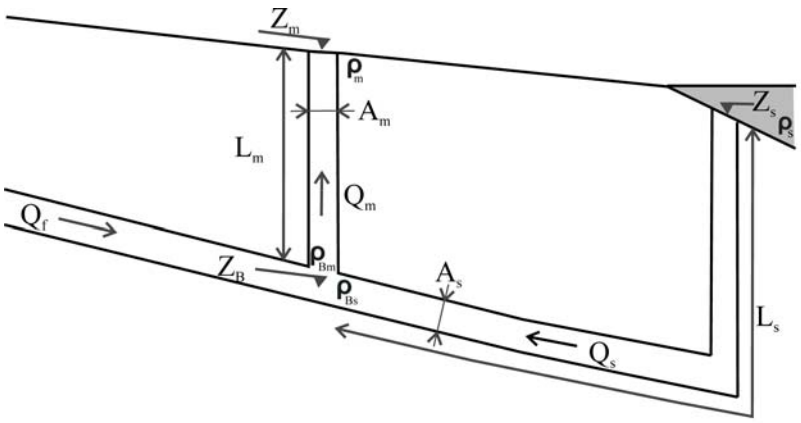

Figure 2.3: Scheme of the conceptual model for brackish springs including the definition of symbols and notations used in the text

2.2. Methods

2.2.1. TURBOCODE solver

The above equations have been solved using an iterative algorithm (called TURBOCODE) programmed in FORTRAN. The procedure is as follows:

1) Initialization. Read $Q_f(t)$, z_{spring}, z_s, z_B, L_m, L_s, n_s (or k_s), n_m (or k_m), A_s, A_m.

Time loop. For each time step perform the following operations.

2) Assume initial value for Q_s (by default, the value at the previous time step).

3) Using Q_f and eqs (2.12), (2.13) and (2.10), obtain Q_m, c_m and ρ_m.

4) Solve transport using eq (2.9) by means of a particle tracking method. Once the spatial distribution of concentrations is known, compute $\overline{\rho}$. Repeat for the seawater and mixed water conduits.

5) Compute H_{Bm} and H_{Bs} using eq (2.15) and (2.16), or eq (2.17).

6) If $H_{Bm} \approx H_{Bs}$, go to next time step. If $H_{Bm} > H_{Bs}$, reduce Q_s (otherwise, increase Q_s), and go to step 3.

2.2.2. Model settings

Simulations were first performed under steady-flow conditions of constant input freshwater flow to facilitate the understanding of the physics of the problem without memory effects. Transient simulations with a time-dependent freshwater input flow were used later to reproduce the actual functioning of brackish springs. The parameter values used in the simulations are listed in Table 2.1. They do not respond to any particular brackish spring but were selected partly from literature values for this type of system and partially from S'Almadrava spring

(Mallorca, Spain). The elevation of the spring mouth is located at +8 m.a.s.l. for all the simulations. The salt mass fraction of freshwater was defined as 6.74×10^{-4}.

Table 2.1: Parameter values used in the steady-flow and transient simulations, for Turbulent-Porous (T-P) and Turbulent-Turbulent (T-T) conceptual models.

	Steady-flow T-P model	**Steady-flow T-T model**	**Transient T-T model**
k_s	1.0×10^{-6}	x	x
L_s	2200.0	2200.0	2200.0
A_s	35.0	0.5	0.5
n_s	x	1.5×10^{-2}	1.5×10^{-2}
z_s	x	x	700.0
z_B	540.0	540.0	540.0
A_m	2.0	2.0	2.0
n_m	1.5×10^{-2}	1.5×10^{-2}	1.5×10^{-2}

2.3. Results and discussion

2.3.1. Freshwater-Seawater mixing ratio at the conduit branching

Discharge rate and concentration of a brackish spring result from the mixing ratio of fresh and seawater at the conduit branching. Therefore, understanding such mixing becomes crucial for predicting the spring response to a certain rainfall event (i.e., freshwater income from the aquifer). For a given freshwater flow rate entering the conduit branching, the phenomenon can be viewed as a mass and energy (or momentum) balance problem. To understand this balance, we first calculate the energy (H_{Bs}) at the conduit branching that results after losses along the seawater conduit as a function of seawater flow (Q_s) coming from the sea. This energy is compared to H_{Bm} (eq 2.15), the energy needed to bring the flow rate resulting from the mixing mass balance to the spring mouth. The problem is resolved when both energies become identical (eq 2.14). In fact, this is the way TURBOCODE operates. We consider steady-flow conditions, i.e., a constant density in every conduit, for discussion simplicity.

Results are shown in Figure 2.4a for the T-P conceptual model with small Q_f. H_{Bs}, the energy at the conduit branching as seen from the sea side, decreases linearly with seawater

flow rate because energy loss at the seawater conduit obey Darcy's law. This relationship is specific to the seawater conduit and does not depend on how much freshwater is flowing into the system. By contrast, the energy necessary to push a column of mixed water towards the spring mouth, H_{Bm}, depends on both fresh (Q_f) and seawater (Q_s) flow rates at the conduit branching. For any given Q_f, this energy increases with Q_s both because friction and the density of the mixture (and thus the weight of the water column) increase with the mixing ratio. For a low Q_f (e.g., 0.25 m^3/s, Figure 2.4a), energy loss in the conduit are small and the dominant term controlling the overall energy is the weight of the water column (eq 2.5). Further, when Q_s tends to zero, the energy necessary is the same that the weight of the mixed water column from the conduit branching to the spring mouth. For higher Q_f, we find that less energy is necessary to push up the same Q_s (Figure 2.4a). This reflects the fact that energy is most sensitive to the density of the mixed water in the vertical column. Density decreases as does H_{Bm}. In fact, for the case of null seawater, the energy necessary is virtually insensitive to Q_f. This is attributed to the fact that, for small Q_f the energy loss in the vertical conduit is also small and the energy required to push the mixed water up depends only on the weight of the water column. And the water column weight will be the same for any Q_f when Q_s is near zero (Figure 2.4a).

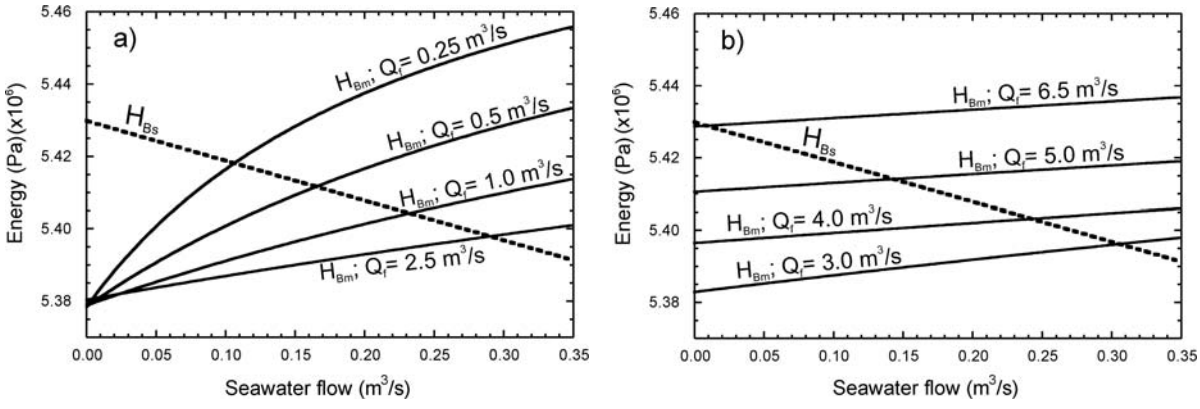

Figure 2.4: Relationship of energy per unit volume computed at the branching point, as seen from the seawater conduit (H_{Bs}) and the mixed water conduit (H_{Bm}) versus seawater flow rate for a) a range of 0.0–3.5 m3/s of freshwater flow rate; and b) a range of 3.0–6.7 m^3/s of freshwater flow rate. Results correspond to steady-flow simulations of Turbulent-Porous conceptual model (Table 2.1).

The situation is different for large Q_f (Figure 2.4b). Energy loss associated with flow resistance in the upwards conduit become increasingly important. In fact, above a critical Q_f,

around 2.5 m^3/s for this example, energy loss become more important than density effects. As resistance increases quadratically with the flow rate of the mixed water (eq 2.7), the energy necessary to allow the mixed water to ascend increases as well. It should be noted that the increase in energy needed to compensate the resistance of the wall of the conduit is not very sensitive to Q_s because the proportion of Q_s in the total spring discharge is minor compared to that of Q_f.

Every point in which two energy lines cross in Figure 2.4 represents a solution of the problem, i.e., energy equilibrium points indicating steady freshwater-seawater ratios at the conduit branching (eq 2.14). Equilibrium occurs with increasing seawater flow rates for increasing Q_f, below the freshwater critical value (Figure 2.4a), but with decreasing Q_s when Q_f is above the critical value (Figure 2.4b). The overall trend is represented in Figure 2.5a. The freshwater-seawater curve is particular for every brackish spring and it is representative of the dimensions of the karst system and the physics of seawater contamination at depth. This critical Q_f value (around 2.5 m^3/s in Figure 2.5a) separates the conditions in which the system is controlled by the weight of the water column, and by energy loss. Note that for even higher Q_f values (higher than 6.7 m^3/s, in this example) the energy equilibrium at the conduit branching is reached for energies higher than the hydraulic pressure of seawater at the conduit outlet to the sea. When this happens, negative Q_s occurs, i.e., groundwater flows from the conduit branching towards the sea, and a submarine spring is created. This situation will be addressed in detail below.

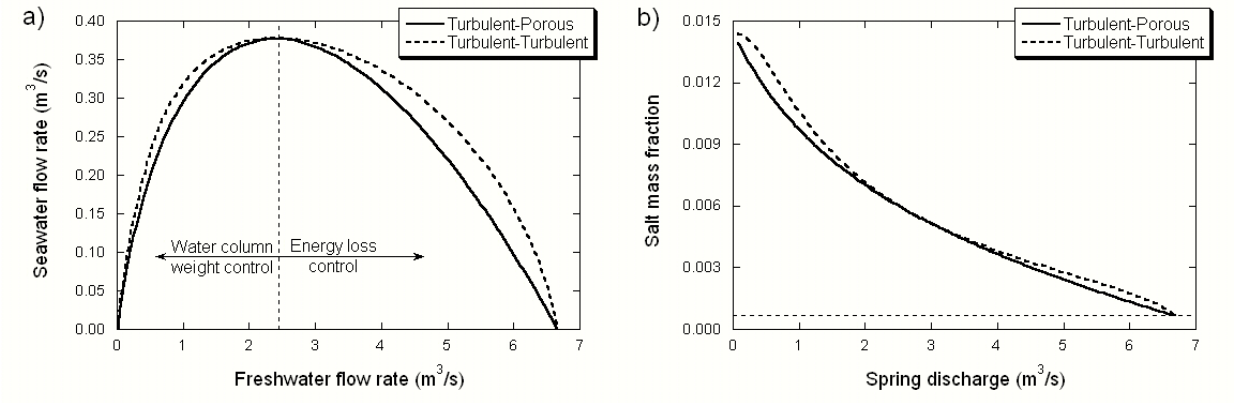

Figure 2.5: Comparison of simulation results for steady-flow simulations of Turbulent-Turbulent and Turbulent-Porous conceptual models (Table 2.1). a) Curves of freshwater-seawater ratio at the conduit branching. The ranges of freshwater flow rate for which the freshwater-seawater ratios are dominated by the weight of the water column or by the energy loss due to resistance are indicated. b) Relation of salt mass fraction and spring discharge. Horizontal dashed line in the plots on the right marks the pure freshwater salt mass fraction in the simulations.

Figure 2.5b shows the relationship of salt mass fraction and the spring discharge. The relation reproduces the freshwater-seawater curve discussed above with an increase on the salinity of the discharge with the flow rate.

For the T-T conceptual model, energy at the conduit branching as measured from the seawards side (H_{Bs} in eq 2.16) no longer depends linearly, but quadratically, on Q_s. This energy decreases with Q_s because of quadratic energy loss in the seawater conduit. On the other hand, the energy necessary to push a column of mixed water up towards the spring mouth in the T-T conceptual model is identical to the T-P case because both are solved by eq (2.15). Results for the T-T case also display two ranges of Q_f in which solution is controlled by the weight of the mixed water column, or by the energy loss in the conduit (Figure 2.5a). However because of the differences of the conceptual models in terms of energy necessary for a particular seawater flow to occur, the energy equilibrium at the conduit branching is reached for different freshwater-seawater ratios on each conceptual model. Figure 2.6 illustrates these differences in our examples, for a low and a high Q_f of 0.25 and 4.5 m^3/s. Because the examples chosen to illustrate the two conceptual models were designed to hold the same freshwater-seawater ratio at the Q_f critical value, any equilibrium point for lower or higher freshwater flow will give a lower freshwater-seawater ratio at the conduit branching for the T-P conceptual model with respect to the T-T case (Figure 2.5a).

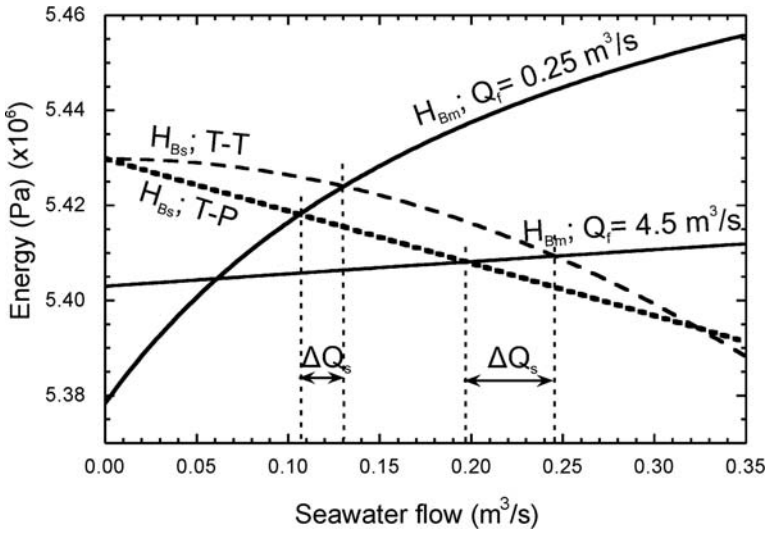

Figure 2.6: Relationship of energy per unit volume computed at the branching point, as seen from the seawater conduit (H_{Bs}) and the mixed water conduit (H_{Bm}) versus seawater flow rate for 0.25 and 4.5 m^3/s of freshwater flow rate. Results correspond to steady-flow simulations of both Turbulent-Porous and Turbulent-turbulent conceptual models (Table 2.1). Single vertical dashed lines mark the energy equilibrium points. Arrows indicate the difference in seawater flow rate for a particular freshwater flow rate, for different conceptual models.

The relation of salt mass fraction and spring discharge in the T-T (Figure 2.5) differs on that obtained for the T-P case near the extreme values of spring discharge. Thus, the salinity of the spring for lower and higher flow rates is increases slightly with respect to that of the T-P to finally end at the same point. This causes a more abrupt relationship for the extreme values that may be used as a distinctive feature of the T-T conceptual model. This will be discussed later.

The two points with zero seawater flow in the curve of freshwater-seawater ratio deserve further discussion. After eqs (2.6), (2.15) and (2.16) or (2.17), Q_s tends to zero for a particular high value of Q_f and when Q_f approaches zero (Figure 2.5a). When the freshwater inflow from the aquifer decreases to zero, the seawater intrusion at the conduit branching also decreases but in a lesser degree. As a consequence, the density of the mixed water flowing up towards the spring mouth increases as does the weight of the water column connected to the spring mouth. Eventually, energy loss and kinetic terms become negligible. Ignoring all velocity dependent terms in eqs (2.15) and (2.16) or (2.17) yields

$$\rho_m L_m = -\rho_s z_B \tag{2.18}$$

which demonstrates that the weight of seawater at the branching point equals the weight of the mixed water column. This expression allows us to derive the elevation of the branching point from the elevation of the spring mouth and the concentration for extremely low flow. In fact, using eq (2.10) for ρ_m and ρ_s and $L_m = z_{spring} - z_B$ yields

$$z_B = \frac{z_{spring}}{1 - \exp\left[\alpha\left(c_s - c_m\right)\right]} \tag{2.19}$$

where z_B is negative because $c_m < c_s$. It is also worth pointing that, in the T-T case, all ignored terms depend on Q^2. Therefore, concentration at the spring mouth should tend to a constant value as Q tends to zero. That is

$$\left.\frac{\partial c_m}{\partial Q}\right|_{Q=0} = 0 \tag{2.20}$$

which explains why c_m becomes constant for small Q in the T-T graph of Figure 2.5b.

On the contrary, for the T-P case the concentration at the spring mouth decreases linearly with Q for small Q (Figure 2.5b). In fact, equating H_{Bm} (eq 2.15) and H_{Bs} (eq 2.17) and taking derivatives yields

$$\left.\frac{\partial c_m}{\partial Q}\right|_{Q=0} = -\frac{\mu L_s}{\rho_m g k L_m} \tag{2.21}$$

which suggests that hydraulic resistance of porous conduit could be derived from the slope of the c_m vs Q graph.

In addition to the spring behaviour at extreme low discharges, Figure 2.5 shows that the solution for medium spring discharges is similar in both conceptual models studied, although the pattern is more linear for the T-P case. This behaviour is also suggested from the freshwater-seawater curves in Figure 2.5a. Finally, the solution for high discharges shows that the T-P case presents a linear relationship of concentration and discharge while the T-T case shows an abrupt ending.

For our example, representing a brackish spring with a spring mouth at 8 m.a.s.l. and a conduit branching at -540 m.a.s.l. (Table 2.1), we obtain a maximum potential salt mass fraction at the spring mouth of 1.4x10-2 (equivalent to 38% of seawater). The grey area in Figure 2.7 illustrates all freshwater-seawater ratios out of the calculated potential range, i.e., it shows ratios that would never be measured in our modeled brackish springs. As expected, for any conceptual model considered, the solution fits the maximum potential freshwater-seawater ratio for very low Q_f values. As the Q_f increases the solution separates from that potential ratio given that the energy loss becomes more significant. It should be pointed out that the dependence of Q_s on Q_f is more linear in the T-T case than in the T-P case. This is attributed to the fact that H_{Bs} remains essentially constant for very low Q_s, Figure 2.6). This implies that salinity at the spring mouth will tend to a constant value for low flow rates (say, below 0.2 m^3/s in our example) in the T-T case, while it will grow steadily to the same value in the T-P case.

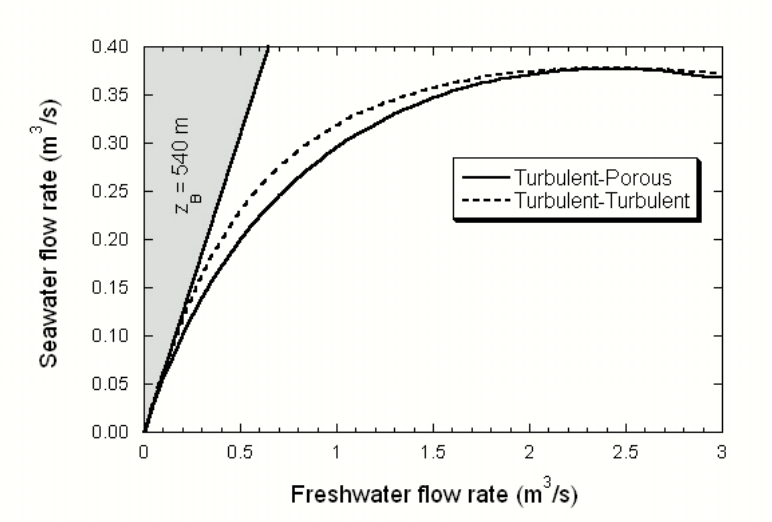

Figure 2.7: Curve of freshwater-seawater ratio at the conduit branching for steady-flow simulations of Turbulent-Turbulent and Turbulent-Porous conceptual models (Table 2.1). The grey area mark freshwater-seawater ratios out of the potential range for the spring mouth elevation and conduit branching depth of the brackish spring simulated.

The second situation with Q_s equal to zero occurs for a particular high Q_f. As discussed before, the energy loss increases quadratically with the mixed water flow and consequently the seawater flow reduces to minimize the concentration of the mixed water, and therefore the weight of the mixed water column. At some point, when the energy at the conduit branching equals the weight of a seawater column, Q_s reaches zero and pure fresh water begins to flow up towards the spring. Although the physical explanation is valid for both T-P and T-T conceptual models, the magnitude of this Q_f is representative of each branching spring and mechanism of salinization (we chose parameters in our example so that this critical value equals 6.7 m^3/s for both conceptual models).

For even higher Q_f, the functioning of the spring is inverted. The energy necessary at the conduit branching to exceed the energy loss in the mixed water conduit is too high to be maintained. As a consequence freshwater starts to flow towards the sea reducing the mixed water flow upwards. The freshwater intruding into the conduit connected to the sea promotes a negative Q_s (i.e., towards the sea) and a submarine spring is produced. Concentration at the spring mouth continues to be pure freshwater while the concentration in the submarine spring mouth is initially that of pure seawater. The functioning of the system changes radically and becomes dependent on the magnitude of the freshwater intrusion into the conduit connected to the sea. In fact, the magnitude of the freshwater intrusion will determine the concentration at the submarine spring, which may even become pure freshwater in an extreme situation. The minimum Q_f where the negative Q_s is produced is essential for a complete characterization of the spring functioning. It marks the flow ranges for which the system behaves as an inland or a submarine spring. Any freshwater-seawater curve for a brackish spring has a theoretical Q_f before the Q_s is inverted, but the Q_f occurring in the aquifer may not be high enough in practice for this situation to occur. Measuring pure freshwater at the spring during high spring discharge periods may confirm that freshwater is intruding into the seawater conduit.

To obtain a more realistic solution to the problem involving submarine springs, equations must be solved in transient-flow mode. Note that for the T-T conceptual model a new parameter must be defined: the depth of the sea outlet (eq 2.16) since the average density in the conduit may no longer be equal to that of the seawater. A time-dependent freshwater inflow function was designed with an increase from 5.0 to 9.0 m^3/s followed by a decrease back to 5.0 m^3/s, with a variation rate of 0.5 m^3/s every 24 hours. This freshwater function was introduced in a T-T simulation type with a sea opening at -700 m.a.s.l. (Table 2.1). Results are shown in Figure 2.8.

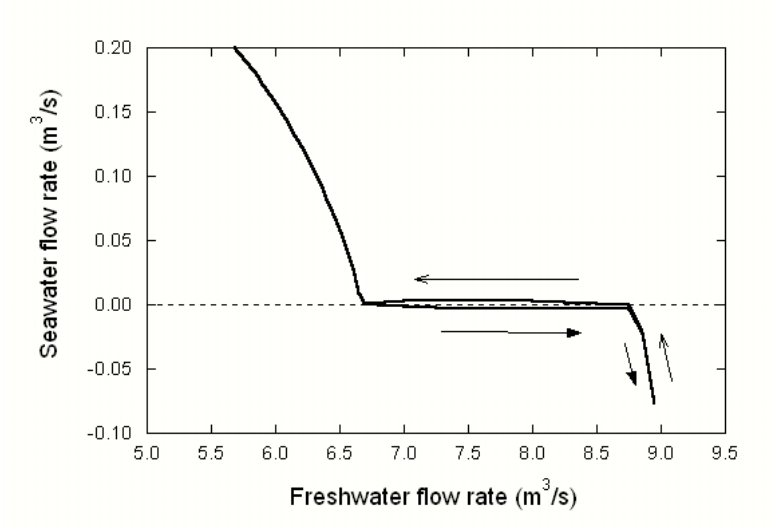

Figure 2.8: Curve of freshwater-seawater ratio at the conduit branching for transient simulation of Turbulent-Turbulent conceptual model (Table 2.1). Arrows indicate the order at which the values are generated when increasing freshwater flow rates (filled arrows) and when decreasing freshwater flow rates (simple arrows). The negative seawater flow rate applies to fluid movement in the seawater conduit towards the sea.

Under these circumstances, the controlling parameters are the depth of the sea outlet and the average density in the conduit connected to the sea (which depends on the length of this conduit and the magnitude of the freshwater intrusion into this conduit). If the depth of the sea outlet is equal or less than that of the conduit branching, the pressure at the sea outlet is less than that at the conduit branching and freshwater is able to intrude easily into the conduit. The submarine discharge will become fresh very quickly, depending on the length of the conduit.

By contrast, if the sea outlet is deeper than the conduit branching, the velocity of the freshwater intruding into the conduit will be very slow. This is due to the double effect of having a higher pressure at the sea opening, and the weight of the water filling the conduit, which is initially pure seawater (Figure 2.8). As Q_f increases, the magnitude of the intrusion becomes more important and the average density of the water in the conduit decreases. At some point, the average density decreases enough to allow the fluid velocity to increase sharply and the submarine spring eventually discharges pure freshwater (Figure 2.8). When Q_f decreases again (e.g., after an important rainfall event) the behavior of the system inverts and the fluid in the conduit becomes positive again (variation of 8.75 to 6.7 m^3/s of freshwater in Figure 2.8). Note that for this range of flow rates, although groundwater flows back towards the conduit branching, the mixed water moving upwards is still pure freshwater. Only when the front of seawater reaches the conduit branching (at 6.7 m^3/s approx., in our example) will the spring discharge become salinized.

2.3.2. Sensitivity analysis

A set of simulations are conducted to illustrate the sensitivity of the spring response with respect to the parameters used in the simulation. First of all, we identify the controlling parameters for each conceptual on steady-flow conditions, from eqs (2.15) and (2.16) or (2.17). Then a perturbation of ±20% is applied separately over the base value of every parameter in order to quantify the relative sensitivity of the solution (Table 2.2). The analysis is performed over steady-flow simulations since it allows to better isolate the effect that each parameter has on the solution. The sensitivity analysis is discussed separately for the two conceptual models. Results are presented in terms of freshwater-seawater ratios and relation of spring discharge and salt mass fraction. These representations are especially useful because they can be compared with the most commonly available field measurements in brackish springs.

Table 2.2: Values of the controlling parameters used in the base simulations for the sensitivity analysis, for Turbulent-Porous (T-P) and Turbulent-Turbulent (T-T) conceptual models. These values were perturbed by ±20% to complete the analysis.

T-P model		**T-T model**	
Parameter	Value	Parameter	Value
A_m (m^2)	2.0	A_m (m^2)	2.0
n_m	1.5×10^{-2}	n_m	1.5×10^{-2}
z_B (m)	540.0	z_B (m)	540.0
$L_s / k_s A_s$ (m^{-3})	$6.3 \times 10^{+7}$	$n_s \sqrt{L_s} / A_s$ ($m^{-2.5}$)	1.41

Turbulent-Porous conceptual model

The solution for a T-P problem depends only on four parameters: A_m, n_m, $L_s / k_s A_s$ and z_B. Although this analysis is performed for steady-flow conditions, these four parameters (plus the history of $Q_f(t)$) would control a transient simulation as well. Figure 2. displays the results (Q_s vs Q_f, and c_m vs Q_m) for the base case and perturbated parameters.

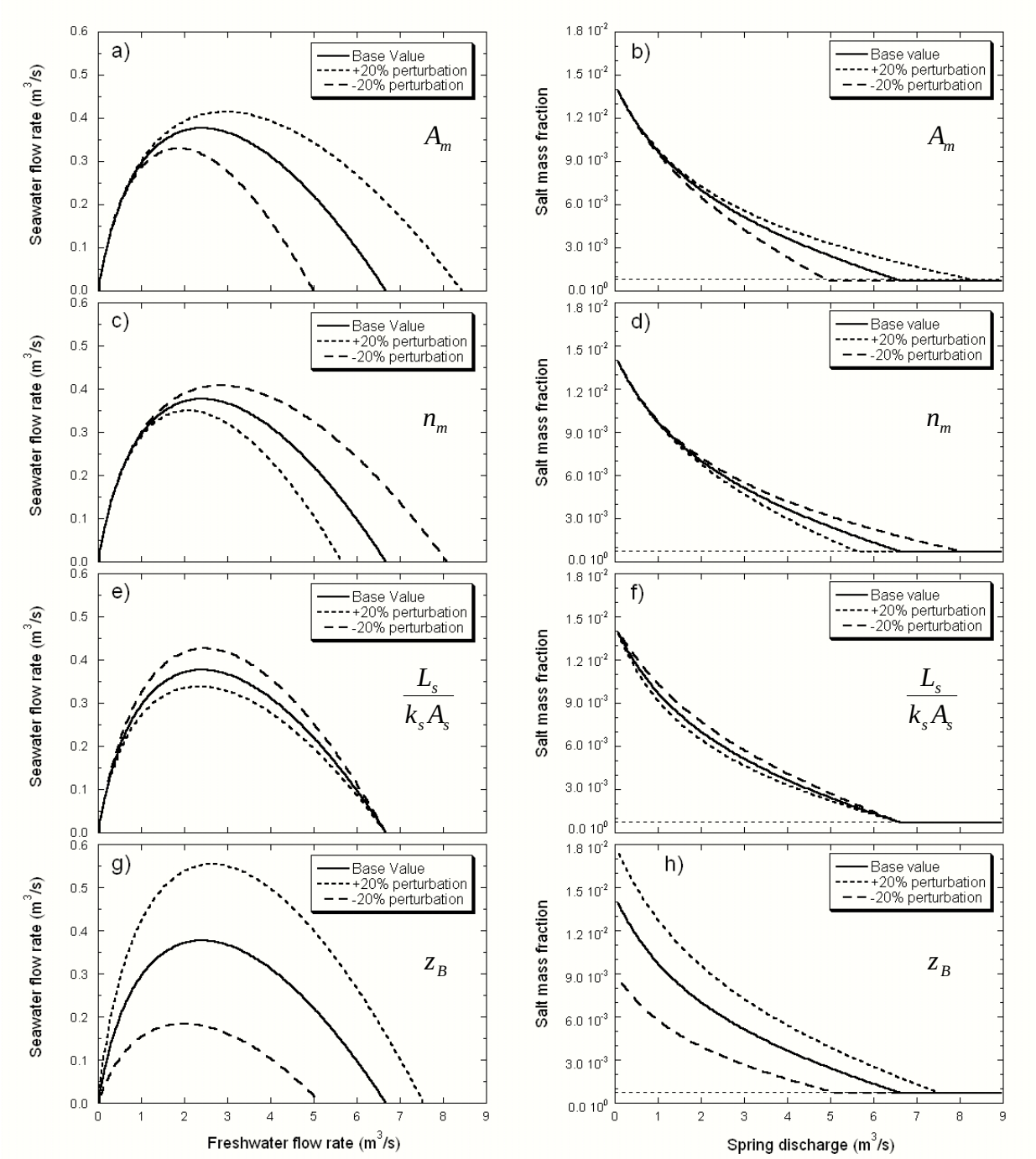

Figure 2.9: Sensitivity analysis Q_s vs Q_f curve (left column) and c_m vs Q_m (right column), with respect to every controlling parameter of the Turbulent-Porous conceptual model: A_m, n_m, $L_s / k_s A_s$ and z_B. Horizontal dashed line in the plots on the right marks the pure freshwater salt mass fraction in the simulations.

The parameters A_m and n_m control the resistance of the vertical conduit to the water flow (eq 2.15) and therefore show a similar –but opposite- influence on the spring response (Figure 2.9a to d). As the energy loss in the vertical conduit is a quadratic function of the water flow, the effect of these parameters is negligible for low Q_f or spring discharges. However, their

influence rapidly increases with Q_f (Figure 2.9a and c). As a consequence, the expected spring concentration will increase with decreasing flow resistance, although this effect can be observed only for high spring discharges. A_m not only controls the energy loss but also the velocity of the groundwater in the conduit, and therefore presents a relatively stronger influence on the spring response than n_m.

The solutions display a negative sensitivity with respect to the parameter $L_s / k_s A_s$ (Figure 2.9e and f), i.e., an increase in the resistance to flow in the seawater conduit reduces the proportion of seawater entering the conduit branching Figure 2.4). Obviously, the solution does not change near the two zero-Q_s situations, which is also consistent with the equations governing the functioning mechanism of the spring. As discussed above, when Q_f approaches zero, the solution only depends on the depth of the conduit branching (eq 2.17) and, accordingly, the solution shows no sensitivity to any other parameter than z_B for this situation (Figure 2.9). For $L_s / k_s A_s$ the solution shows no sensitivity at the other zero-Q_s point because the energy equilibrium for this situation to occur depends on the depth of the conduit branching and on the resistance in the vertical conduit (Figure 2.9, eqs 2.15 and 2.17). For spring discharges exceeding 6.5 m^3/s approx., the spring concentration is pure freshwater, indicating the existence of a submarine spring-like behaviour.

Finally, the depth of the conduit branching, z_B, exerts an influence on the spring concentration for any discharge (Figure 2.9g and h). As discussed above, the proportion of seawater entering the conduit branching increases with z_B because the pressure resulting from the weight of the seawater column increases accordingly. Consequently, the spring salt mass fraction for any spring discharge is higher for deeper conduit branchings (Figure 2.9h). This parameter influences the energy curves of both the seawater and the mixed water conduit (eq(15) and eq(17)). The slope of the freshwater-seawater curve when the freshwater flow approaches zero, is also dependent on the parameter value (recall eq(18), Figure 2.9g). Results also show that shallow conduit branchings will facilicitate the formation of submarine springs because the minimum Q_f necessary to inverse Q_s is smaller.

An analysis of Figure 2.9 suggests that a spring with a broad range of measured discharges could allow us to characterize: (1) the resistance of the upwards conduit (but not n_m and L_m separately) from the response of high flow rate; (2) the depth of the branching point (z_B) from the low flow concentration; and (3) the hydraulic resistance of the seawater conduit from the low flow slope of c_m vs Q_m.

Turbulent-Turbulent conceptual model

The solution for a T-P problem depends on four parameters: A_m, n_m, $n_s\sqrt{L_s}/A_s$ and z_B. Note that, although the solution for transient simulations also depends on the depth of the sea outlet (eq 2.16), the solution would only be sensitive to this parameter when freshwater intrudes into the conduit connected to sea. Therefore, a sensitivity analysis for this parameter should also be performed in simulations seeking to reproduce submarine brackish springs. Figure 2.10 shows the results of the sensitivity of the solution to all the controlling parameters.

Results for this case are generally analogous to those of the T-P case. The most striking feature is that the behaviour at the two zero Q_s points is most sensitive to flow resistance parameters at the seawater conduit.

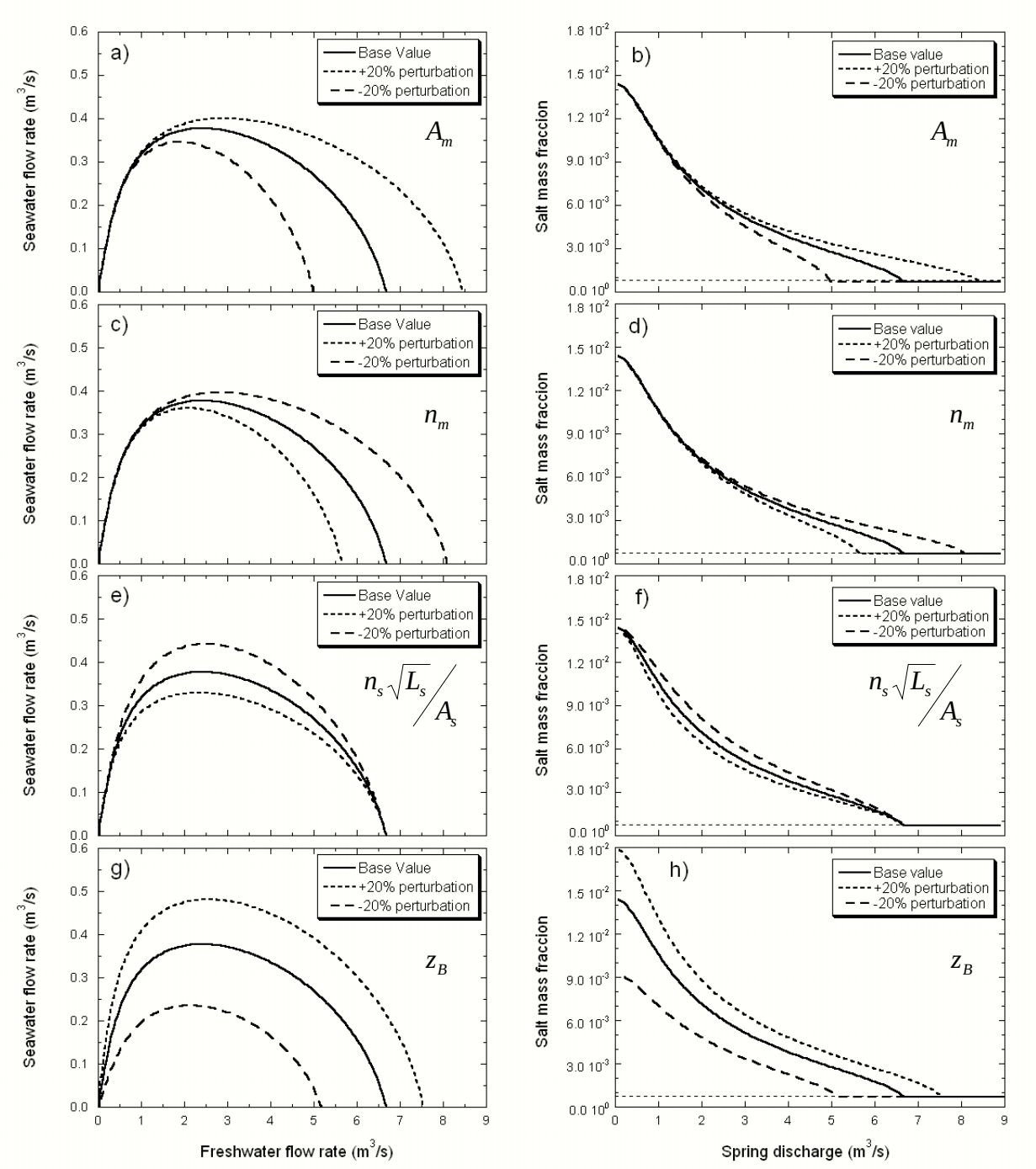

Figure 2.10: Sensitivity analysis Q_s vs Q_f curve (left column) and c_m vs Q_m) (right column), with respect to every controlling parameters of the Turbulent-Turbulent conceptual model: A_m, n_m, $n_s\sqrt{L_s}/A_s$ and z_B. Horizontal dashed line in the plots on the right marks the pure freshwater salt mass fraction in the simulations.

2.3.3. Comparison with field data

The results obtained in TURBOCODE simulations are compared with field data observations from three brackish springs: Almyros of Heraklion spring (Crete, Greece), Pantan spring (Croatia) and S'Almadrava spring (Mallorca, Spain). Figure 2.11 shows the relationship of the spring concentration and discharge for S'Almadrava (Sanz et al., 2002), Pantan (Breznick, 1973) and Almyros (Monopolis et al., 1995). The authors proposed that the salinization of these springs is due to the greater density of seawater in the T-T scheme. Regardless the differences in number of observations and in salinity or discharge ranges, all springs show similar patterns with a decreasing salinity for increasing spring discharges (Figure 2.11). Filed data for S'Almadrava covers a wide range on spring discharges (Figure 2.11a). From these observations, the conceptual model controling the functioning of S'Almadrava spring would be a T-T case because: (1) the relation of salinity and flow rate is far from linearity for medium spring discharges, and (2) for very low discharges, the spring concentration seems to reach a constant value (Figure 2.10, right hand side plots).

The available observations for Pantan spring also covers a wide range of spring discharges and the connection to the sea seems to be controlled for a karst conduit (T-T case) (Figure 2.11b). However, the limited number of data available prevents from further discussion. On the contrary, many observations are available for Almyros spring (Figure 2.11c). Data concentrates for medium to high spring discharges, were the spring clearly discharges freshwater. Field measurements seem to form a curve of high linearity. This observation is more consistent with a T-P case (Figures 2.5b and 9). However, the distinction of the conceptual model of Almyros turns out to be difficult due to the lack of data for very low flow discharges.

The fact that the field measurements show some spreading with respect to the simulated curves for steady-flows presented in this study could be attributed to the memory effects resulting from the dynamic nature of the systems or be a consequence of the higher complexity of the karst network in the aquifers (e.g., multiple conduit branchings), compared with the simplifications considered in this study.

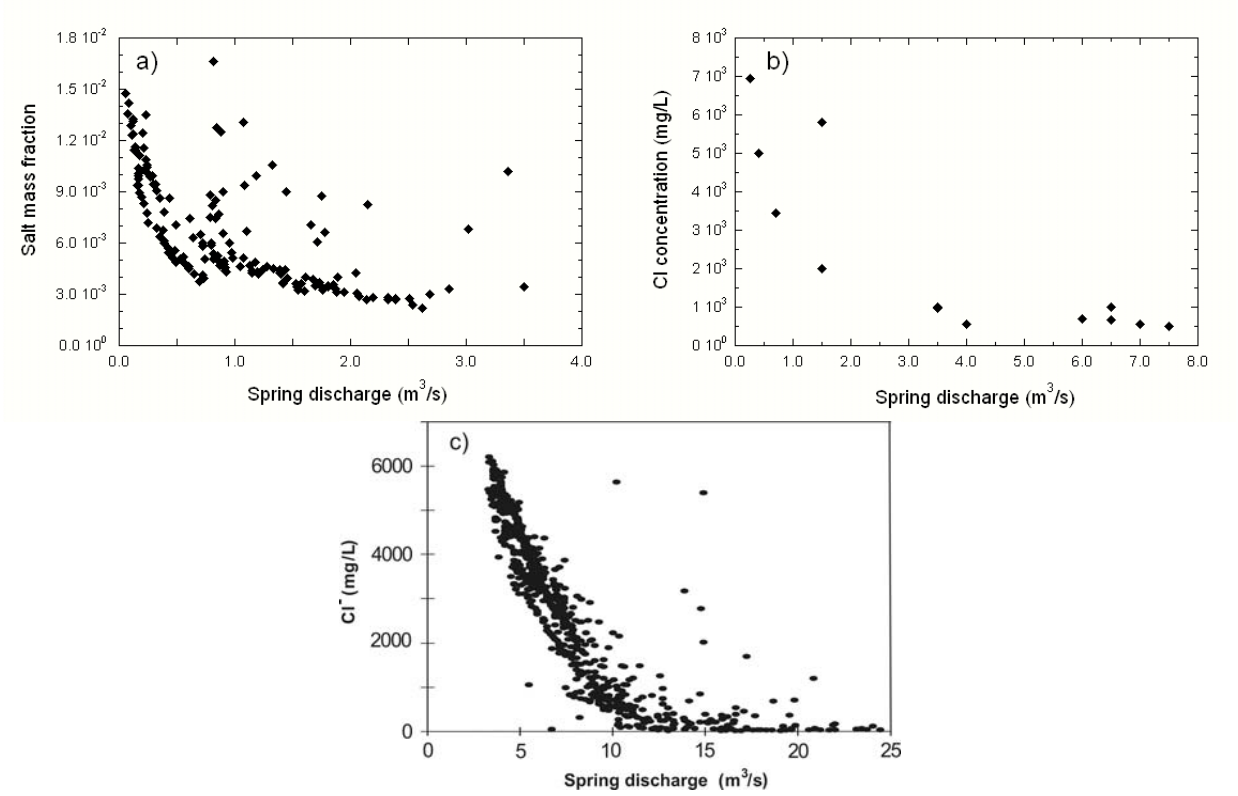

Figure 2.11: Relationship of spring discharge and water quality for a) S'Almadrava spring (Mallorca) (after Sanz et al. 2002); b) Pantan spring (Croatia) (after Breznick, 1973); and c) Almyros spring of Heraklion (Crete) (after Monopolis et al, 1995)

The freshwater-seawater ratios from field measurements in S'Almadrava spring and Almyros spring (Maramathas et al., 2006) are shown in Figure 2.12. The data from S'Almadrava spring shows a zero-Q_s point for Q_f approaching zero. The freshwater-seawater ratio then increases linearly with Q_f before gradually stabilizing in about 0.15 m^3/s of Q_s for a wide range of Q_f. This pattern agrees with simulations of this study for T-T conceptual model (Figure 2.5a and Figure 2.10, left hand side figures). The field data for this spring does not show any significant decrease in Q_s for higher Q_f, and therefore Q_f of at least 4 m^3/s are expected to be necessary for the formation of a submarine spring.

Field measurements for Almyros spring form a curve with an abrupt decrease in Q_s with Q_f until a zero-Q_s point is reached for about 5.6 m^3/s Q_f. Null seawater contribution (that is, pure freshwater discharging at the spring) is maintained for even higher Q_f, in line with the formation of a submarine spring at the sea bottom predicted in our simulations (Figure 2.8). The formation of submarine springs may be reconcilable with either T-T or T-P conceptual models and we would need more geology information to confirm any conceptual model. Despite, the abruptness of the freshwater-seawater curve when approaching the zero-Q_s point indicates that a T-T scheme is more likely to be occurring at Almyros. The different interpretations that may arise

from the available observations for Almyros spring point out the difficulty of selecting the conceptual model governing brackish springs. This is especially so when the available observations do not cover a wide range of spring discharges including the two zero-Q_s points. In fact, Arfib and de Marsily (2004) and Maramathas et al., 2003, built numerical simulations describing the T-P and T-T conceptual models, respectively, and obtained reasonable results in both cases.

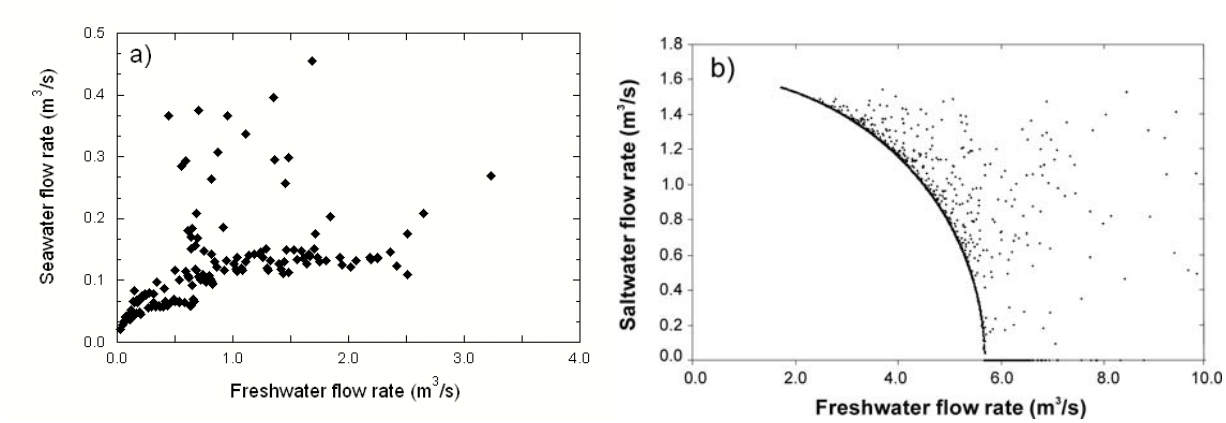

Figure 2.12: Freshwater-seawater ratio relationship for a) S'Almadrava spring (Mallorca, Spain); and b) Almyros of Heraklion spring (Crete, Greece) (after Maramathas et al., 2006).

2.4. Conclusions

In this study we use simple hydraulic models to reproduce the basic physics controlling the salinization of brackish springs. The equations governing turbulent flow for variable-density fluids are derived and solved with an iterative algorithm programmed in FORTRAN (called TURBOCODE). The solution has been found for systems consisting of a deep mixing place in which a freshwater conduit and another conduit connected to the sea join a third conduit with mixed water leading to the spring mouth. Two conceptual models have been tested: the Turbulent-Turbulent case in which the conduit salinization comes from a karst conduit connected to the sea, and the Turbulent-Porous case in which the seawater intrusion occurs through a fissured matrix (Figure 2.1 and Figure 2.2, respectively). In both cases flow is governed by mass and either momentum or energy conservation. The response of the spring concentration to the variation of freshwater flow rate from the aquifer is evaluated in steady-flow conditions in terms of energy balance at the mixing point and freshwater-seawater ratios. For low freshwater flow rates, the spring response is controlled by the weight of the water column flowing towards the spring mouth. As the freshwater flow increases, the energy loss increases and the resistance of the walls to flow becomes the controlling factor for high freshwater flow rates. Results are similar for both conceptual models for medium spring discharges, although

the dependency of spring salinity with discharge is more linear for the Turbulent-Porous case. Additionally, for very low spring discharges, the concentration for the Turbulent-Turbulent case becomes constant when the spring discharge tends to zero. This points out that, for this situation the solution depends only on the water column weight in the vertical conduit. In fact, the spring dries up when the excess in elevation of the spring mouth is balanced by the excess in of density of seawater with respect to that of the mixed water in the conduit connected to the spring mouth. The depth of the conduit branching can be then approximated from the elevation of the spring mouth and from spring salinity for very low spring discharges.

The sensitivity of the spring response with respect to the parameters controlling the system is also evaluated in terms of freshwater-seawater ratios and the relation of spring discharge and salt mass fraction. For the Turbulent-Porous case, the simulation is sensitive to A_m and n_m for high freshwater flow rates, but their effect is opposite: salinity increases for larger A_m and smaller n_m. This is attributed to the quadratic increase of energy loss in the vertical conduit with the spring discharge. The solution for medium freshwater flow rates depends on $L_s / k_s A_s$. A higher parameter value increases the energy loss of the seawater intruding into the aquifer and thus reduces the salinitzation at the conduit branching. Finally, for low freshwater flow rates the solution only depends on depth of the conduit branching since it controls the limiting water column weight that the system can support before the spring dries up. The sensitivity of the solution in the Turbulent-Turbulent case is very similar to that for the Turbulent-Porous one for the parameters A_m, n_m and z_B. The resistance to flow in the conduit connected to the sea can be expressed now as $n_s \sqrt{L_s} / A_s$., where an increase of the resistance not only reduces the proportion of the seawater mixing at the branching point but also the salinity discharging from the spring. This effect is only important for medium freshwater flow rates since the solution for high flow rates is dominated by the energy loss in the vertical conduit rather than in the conduit connected to the sea. If the freshwater flow rate overpasses a limiting value, the high energy loss in the vertical conduit may promote a freshwater intrusion into the conduit connected to the sea. This will generate the formation of a submarine spring in the sea floor of variable density depending on the extent of the intrusion and the depth of the conduit outlet in the sea. This situation may be identified by measuring freshwater concentration during stages of high spring discharges in the spring.

The prediction curves of freshwater-seawater ratio and the relationship of spring discharge and salt mass fraction are compared with field data from Pantan spring, Almyros of Heraklion spring and S'Almadrava spring. The simulation results show a good agreement with the field data available, and provide insights to identify the conceptual model governing every particular springs. The analysis highlights the importance of using field data encompassing the whole range of spring discharges for a sound understanding of the spring functioning.

The freshwater-seawater curve is specific to all brackish springs and it is representative of the dimensions of the karst system and the salinization mechanism. In the light of our findings an analysis based on the freshwater-seawater ratios rather than on the relationship of spring concentration and discharge proves to be more suitable for identifying the salinization mechanisms of some brackish springs.